Supplemental Information for

MixMD Probeview: Robust Binding Site Prediction from Cosolvent Simulations

Sarah E. Graham[†], Noah Leja[‡], Heather A. Carlson[†‡§]*

[†]Department of Biophysics, [§]Department of Medicinal Chemistry, and [‡]College of Pharmacy

University of Michigan, Ann Arbor, Michigan, 48109-1065

* Email: carlsonh@umich.edu

Description: Figure S.1 shows that the initial placement of probes for DHFR solo simulations is not biased to predict the known binding site. (For brevity, only DHFR is shown as an example.) Figures S.2-S.5 give detailed comparisons of the local maxima for all solvent mixtures. Separate, additional files are provided for the MixMD Probeview Python Script (MixMD_Probeview_final.py.txt) and the MixMD Probeview User's Guide (MixMD_Probeview_User_Guide.pdf).

Initial Locations of Cosolvent Probes in DHFR

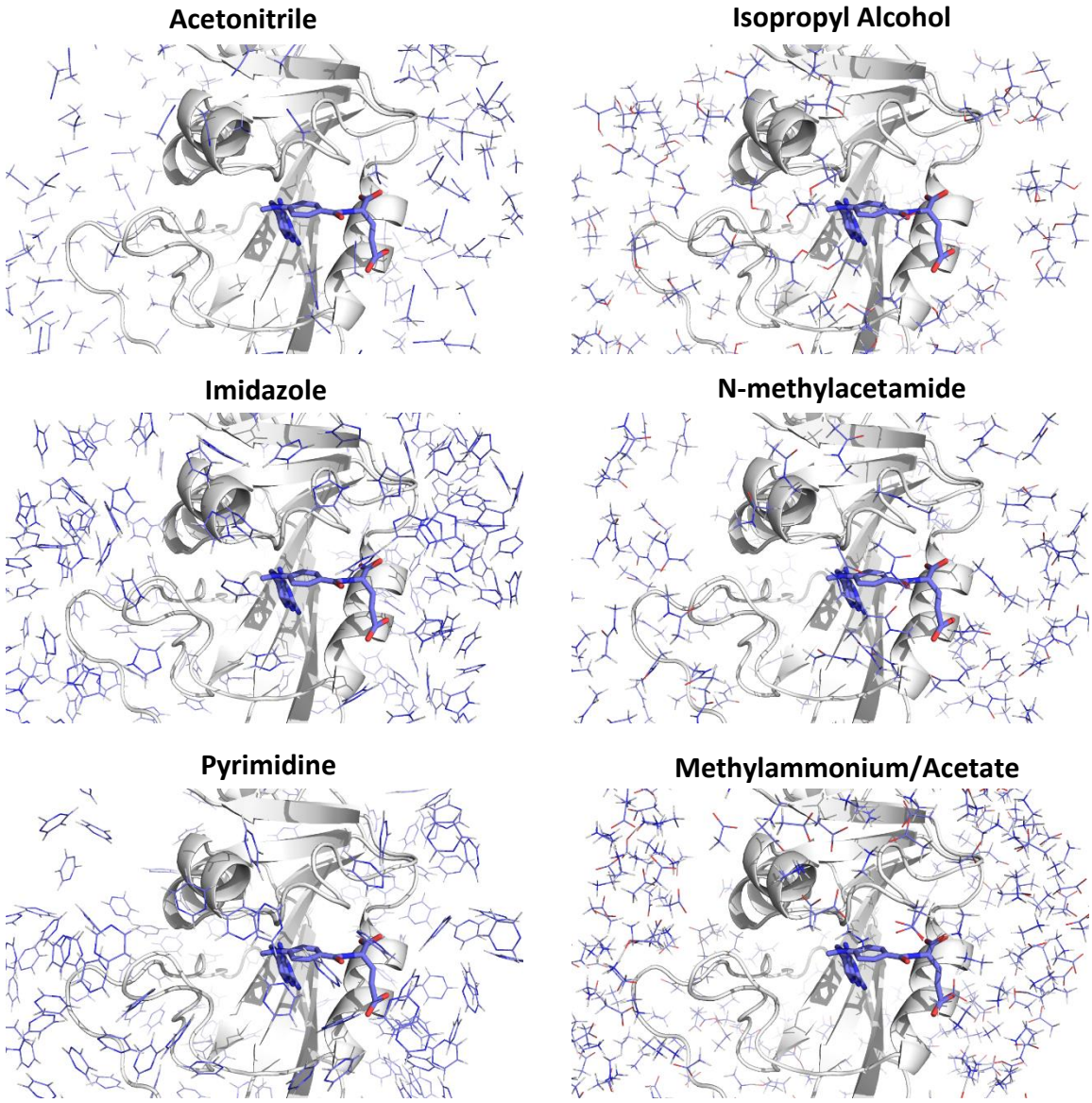

Figure S.1: Starting structures for each of the simulations of single probe types for Dihydrofolate Reductase. Water molecules are not shown. Probes were randomly distributed over the surface of the protein using tleap and were not preferentially placed in any specific region on the protein's surface. Methotrexate (PDB:1DF7) is shown in the binding site for reference.

Local Maxima for Simulations of ABL Kinase

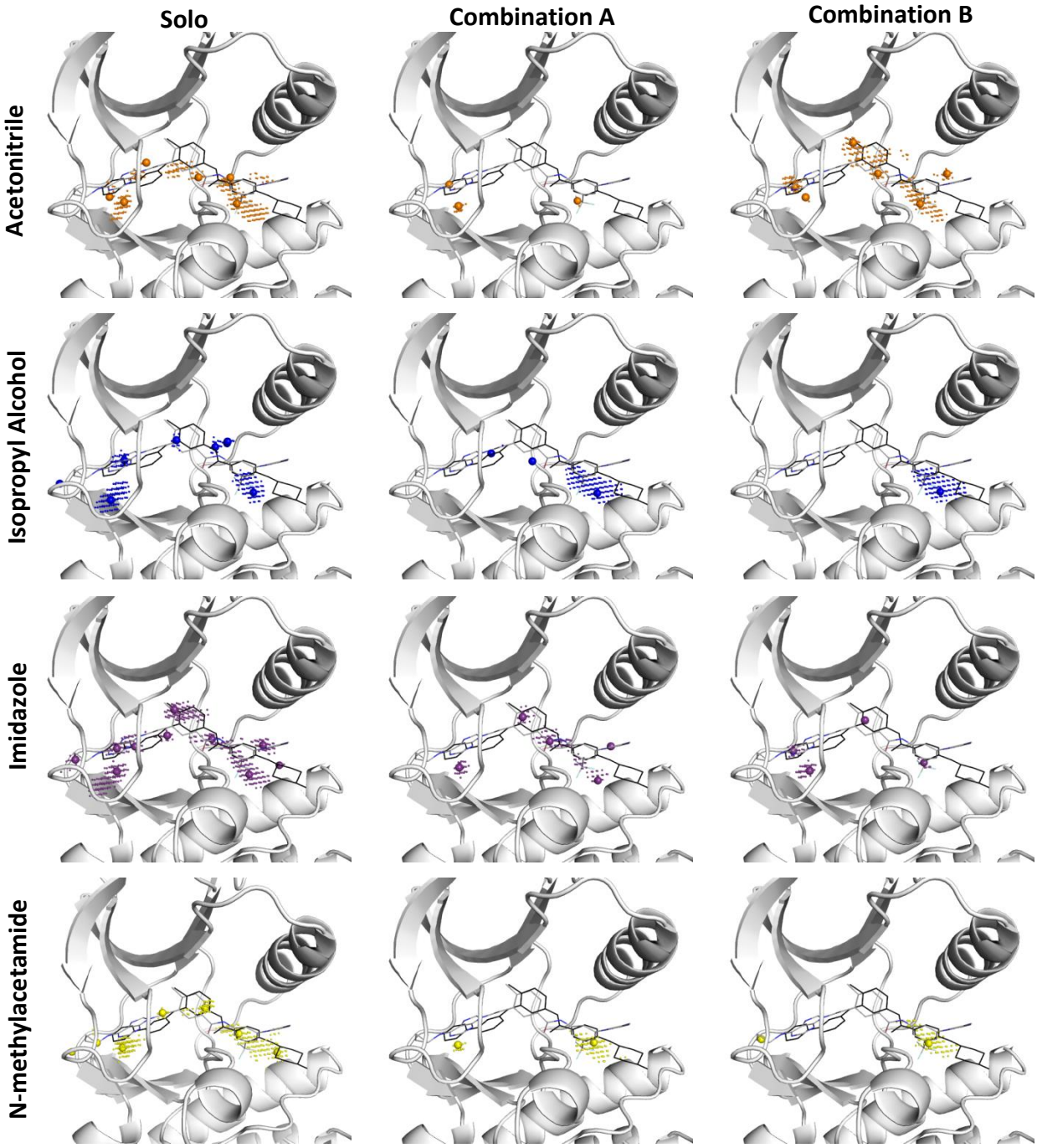

Local Maxima for ABL Kinase, continued

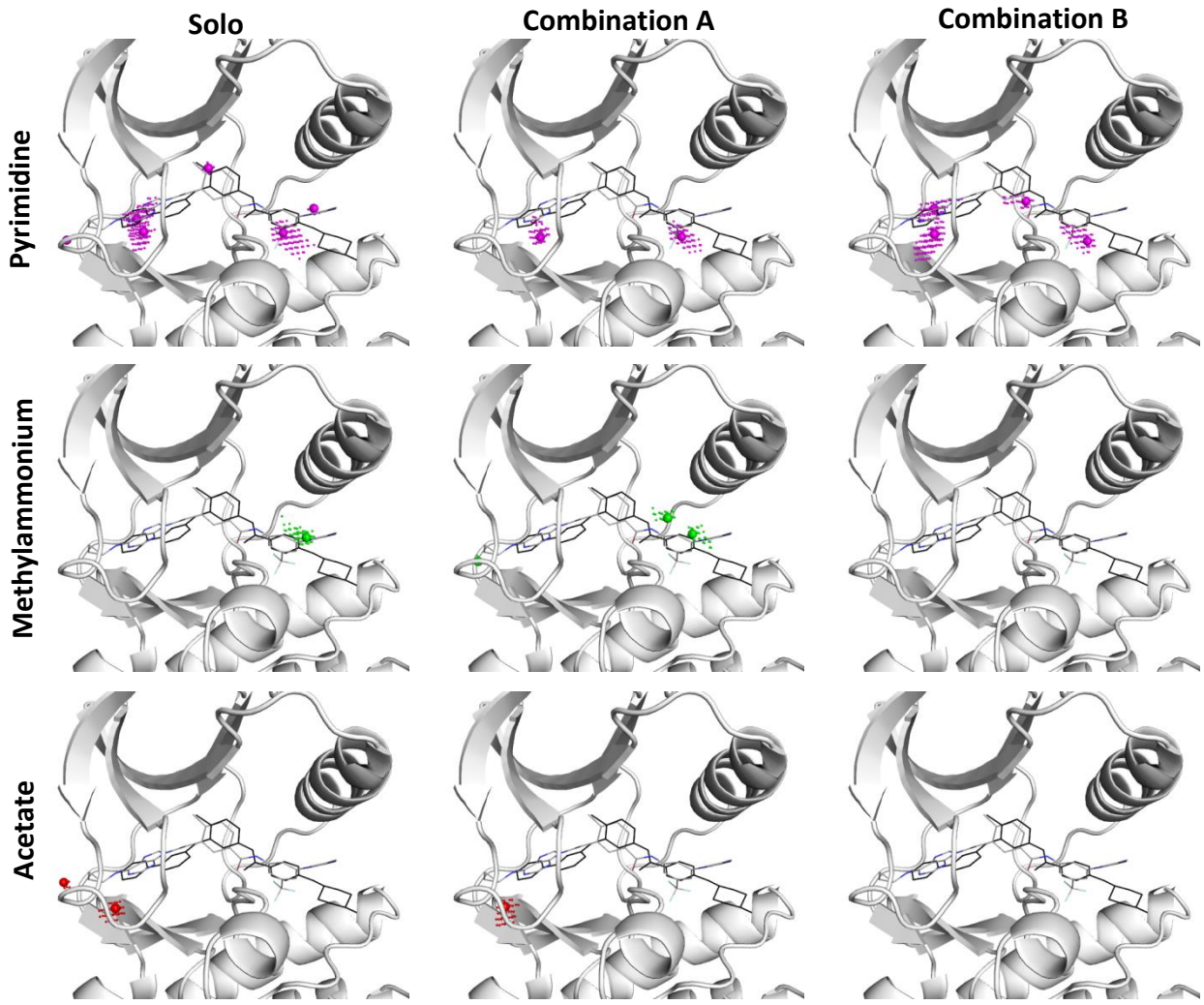

Figure S.2: MixMD Probeview identified the active site as one of the highest ranked hotspots in ABL kinase. Grid points with 10% or greater occupancy within the active site are shown for each solvent across the three MixMD setups. Local maxima are shown as spheres, with surrounding grid points shown. Imatinib (PDB:1OPJ)[1] and B91 (PDB:3KFA)[2] are shown for reference. Solo simulations accurately map the active site region, in agreement with known ligands. Imidazole shows the most extensive mapping, with local maxima corresponding to aromatic portions of the ligands. Solvent combinations A and B map the active site as well, but with fewer local maxima due to competition between solvents. For example, in solvent combination B the N-methylacetamide occupancy seen within the left-hand side of the ligand in the solo simulations is displaced by pyrimidine. This is consistent with ligand-bound structures which place aromatic rings at this site. However, N-methylacetamide serves to identify hydrogen-bonding interactions, which may not be observed if the site is preferentially bound by other probe molecules.

Local Maxima of Androgen Receptor

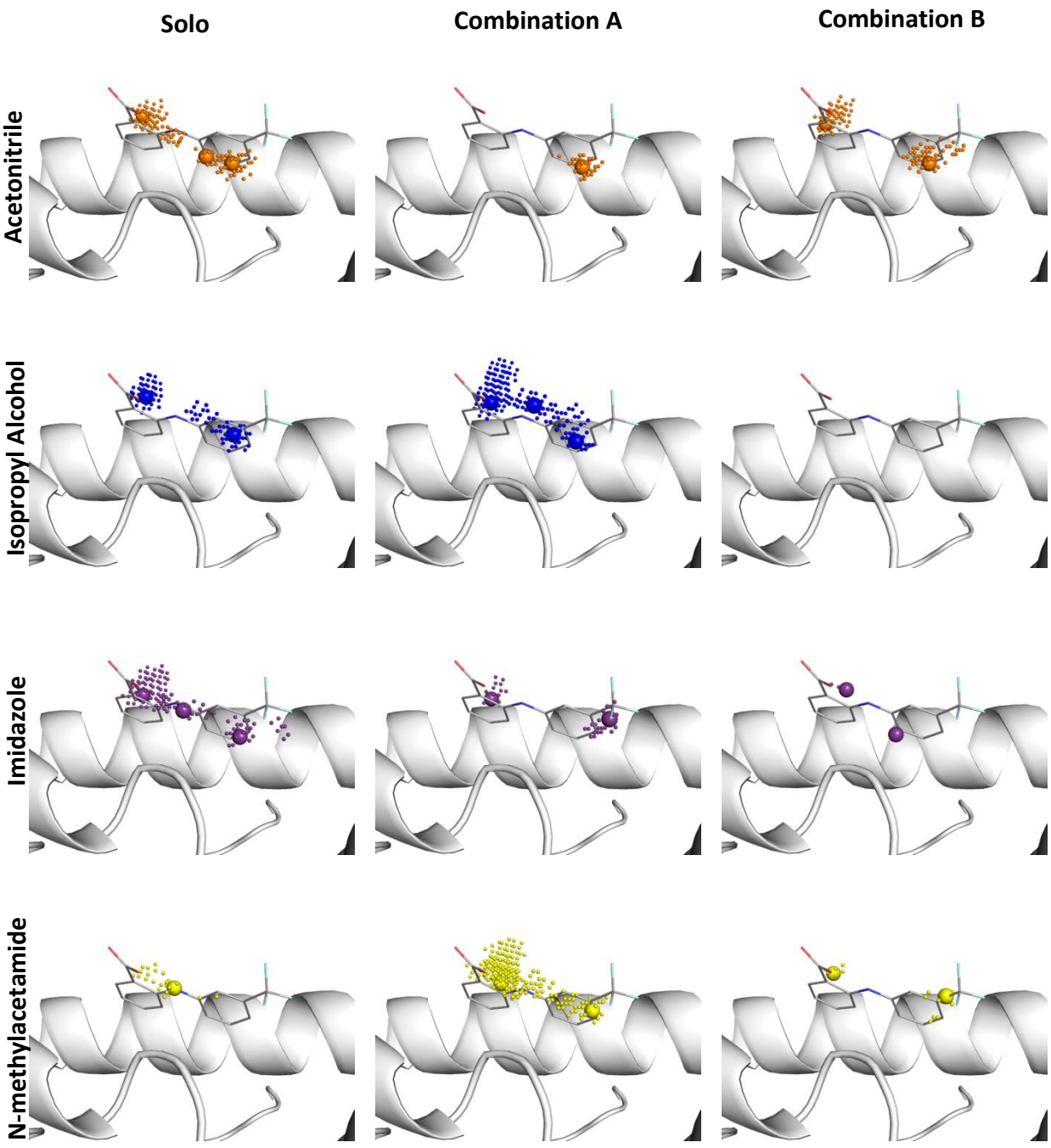

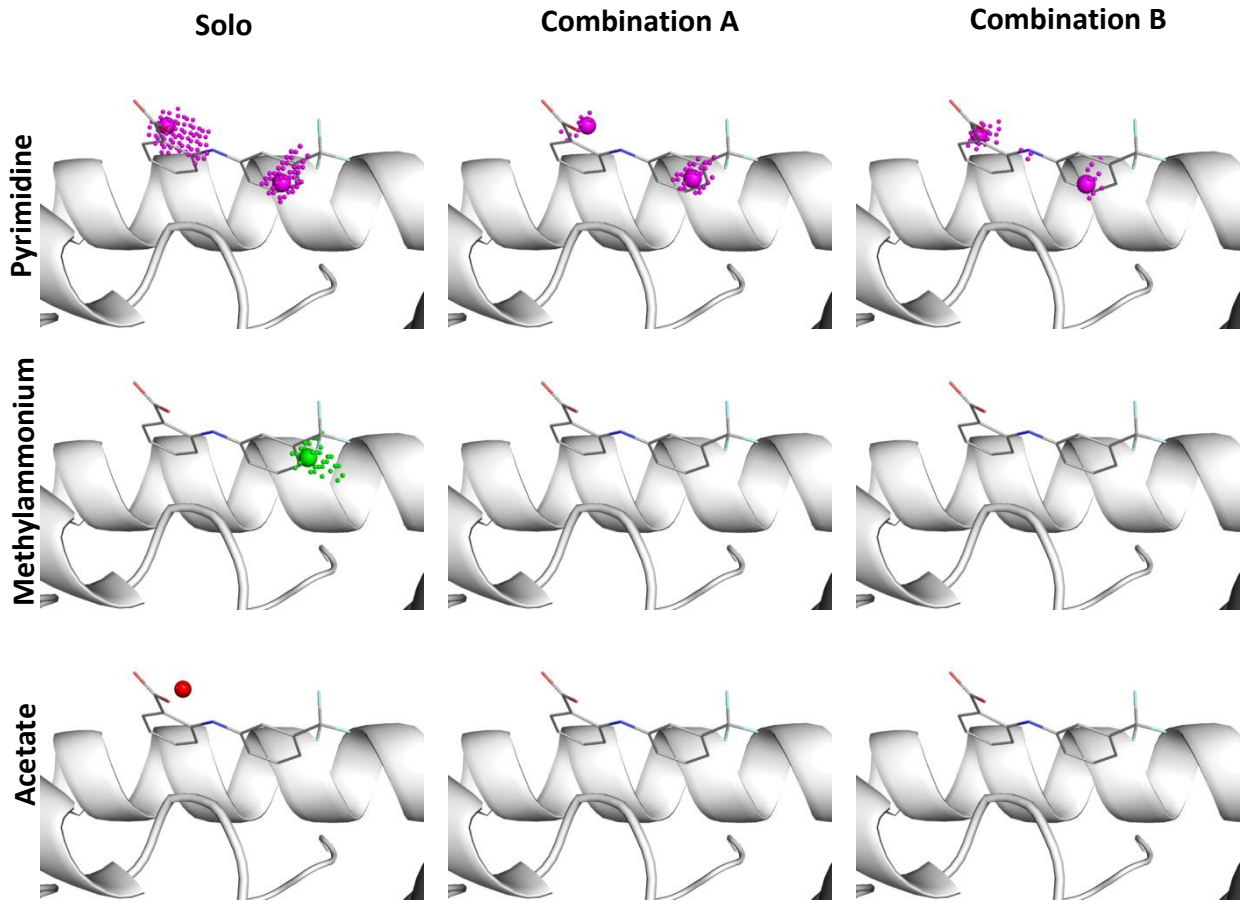

Figure S.3: MixMD Probeview identified the allosteric site as one of the highest ranked hotspots in androgen receptor. Grid points with 10% or greater occupancy within this site are shown for each solvent across the three MixMD setups. Local maxima are shown as spheres with surrounding grid points shown. The active site of AR has minimal solvent exposure, and so differences in sampling between solvent sets are expected. For this reason, we have shown local maxima for one of the allosteric sites. The allosteric site ligand, flufenamic acid (PDB:2PIX)[3], is shown for reference. Solo simulations show each probe accurately maps the allosteric site ligand but with different occupancy strengths. Acetonitrile, isopropyl alcohol, and imidazole all had similar top occupancies for the solo simulations, with the two charged probes, methylammonium and acetate, having the least occupancy. Solvent combinations A and B mirror the solo simulations, but with a few noticeable differences. First, the charged probes fail to map the ligand at all in both solvent combos A and B. This is likely due to the site's preference for other types of interactions, leading to the charged probe's displacement. Isopropyl alcohol shows strong mapping in combination A, whereas in combination B it is displaced by acetonitrile and imidazole. Visualizing the occupancy at lower levels reveals that isopropyl alcohol does sample this site, but is below the 10% cutoff. Additionally, acetonitrile has only one local maximum in solvent combination A, but two in combination B.

Local Maxima of BACE

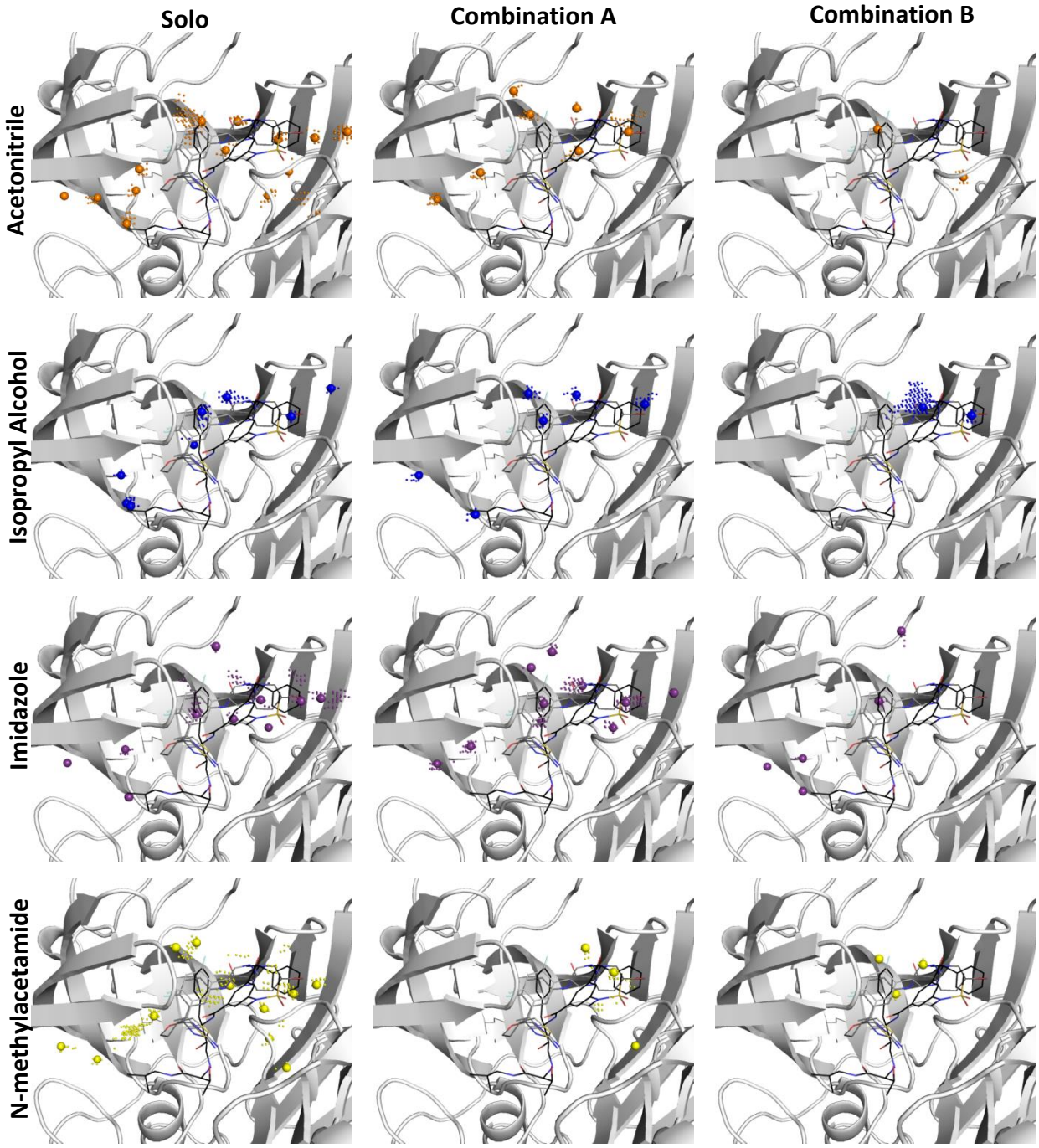

Local Maxima of BACE, continued

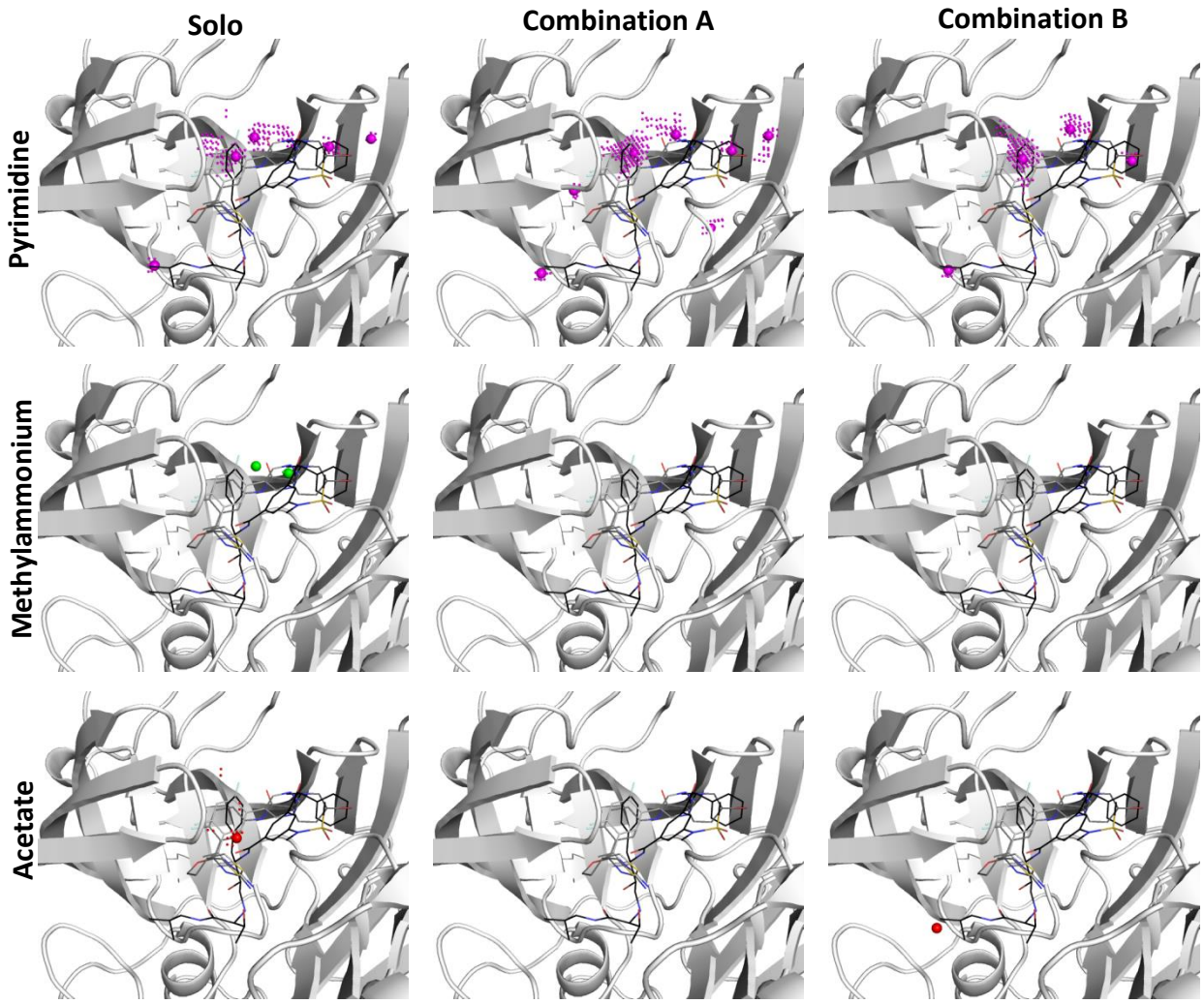

Figure S.4: MixMD Probeview identified the active site as the highest ranked hotspots in BACE. Grid points with 10% or greater occupancy within the active site are shown for each solvent across the three MixMD setups. Local maxima are shown as spheres, with surrounding grid points shown. Ligands LY2811376 (PDB:4YBI, 4B2)[4], 5E7 (PDB:5DQC)[5], and 7H3 (PDB:5TOL)[6] are shown for reference. Solo simulations show each probe accurately mapping the active site in agreement with known ligands. The neutral probes mapped the active site ligand extensively, while the two charged probes, acetate and methylammonium, had significantly less mapping within the site. Solvent combinations A and B mapped the active site similarly to the solo simulations, with the charged probes being the primary difference. In the combined simulations, the charged probes were displaced in favor of the neutral probes.

Local Maxima of DHFR

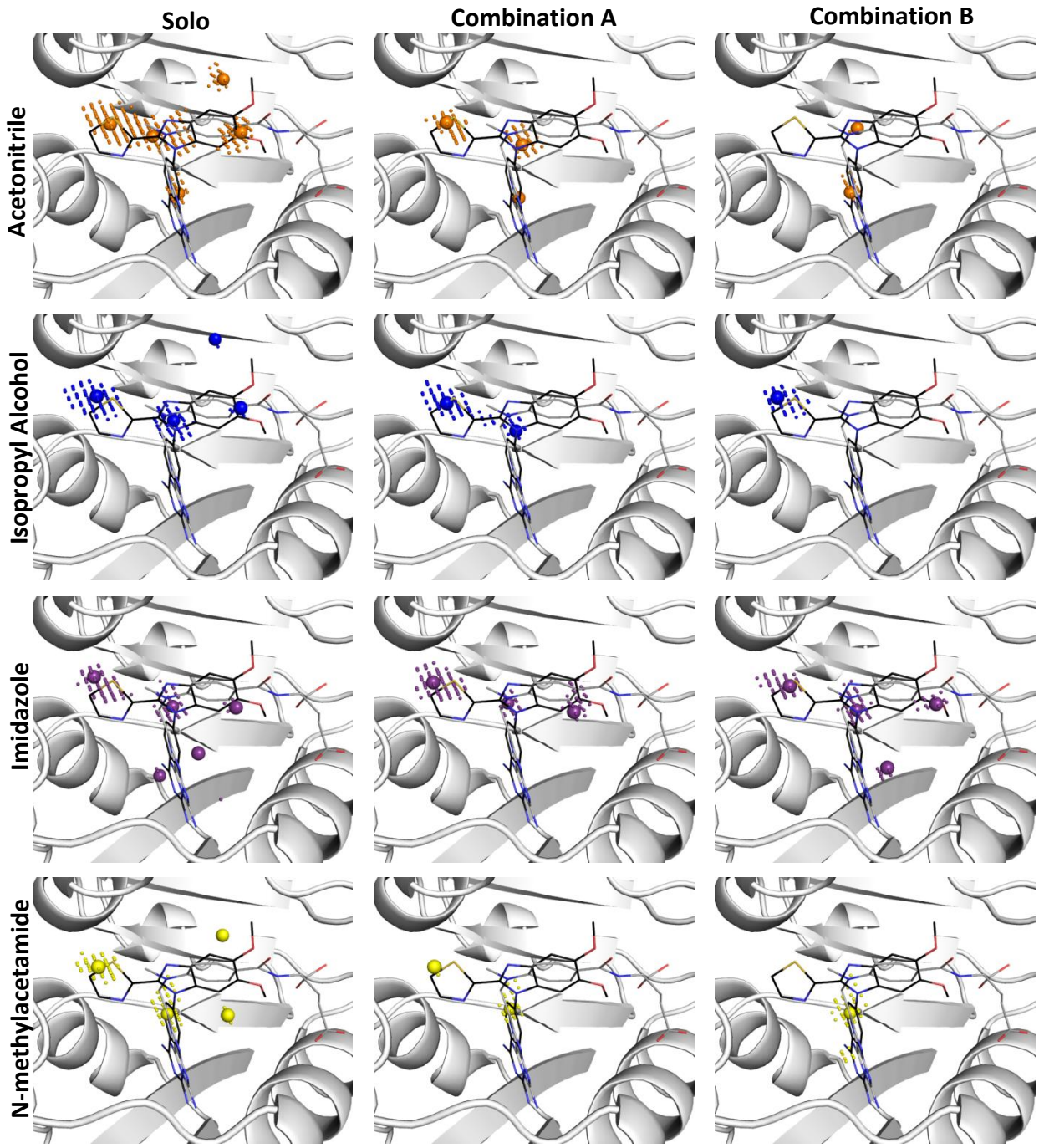

Local Maxima of DHFR, continued

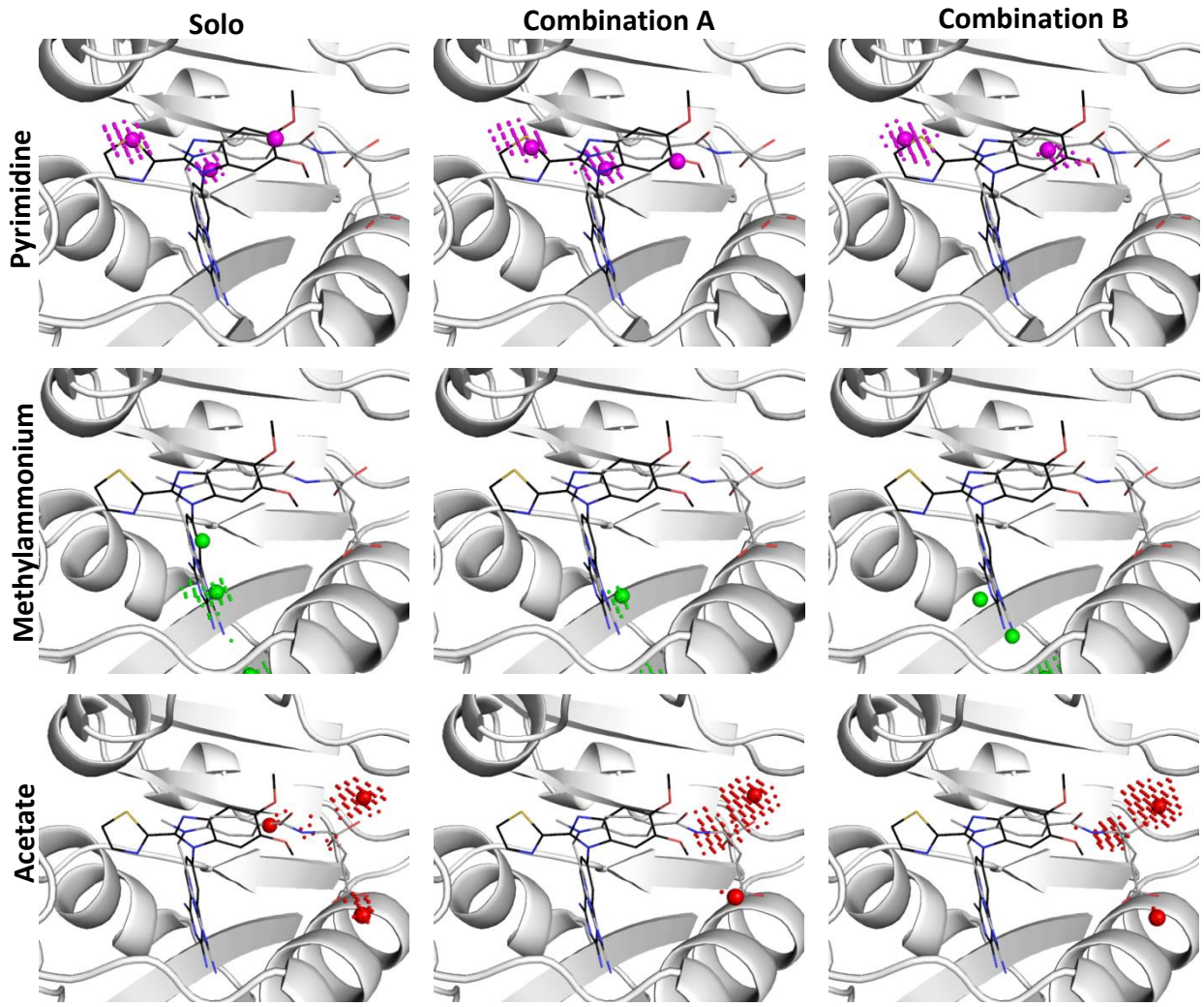

Figure S.5: MixMD Probeview identified the active site as the highest ranked hotspots in DHFR. Grid points with 10% or greater occupancy within the active site are shown for each solvent across the three MixMD setups, with the exception of the charged probes for which nearby sites are shown. Local maxima are shown as spheres, with surrounding grid points shown. Methotrexate and the ligand 1DN are shown for reference (PDB:1DF7, MTX and PDB:4LEK,1DN).[7,8] Mapping of the binding site was similar between all solvents sets, although solvent combination B showed preferential binding to portions of the active-site by acetonitrile and isopropyl alcohol when run in combination with imidazole. The charged probes indicate favorable interactions outside of the core region of the ligand, which mimic the interactions made by the carboxylate groups of methotrexate.

1. Nagar, B.; Hantschel, O.; Young, M. A.; Scheffzek, K.; Veach, D.; Bornmann, W.; Clarkson, B.; Superti-Furga, G.; Kuriyan, J., Structural Basis for the Autoinhibition of c-Abl Tyrosine Kinase. *Cell* **2003**, 112, 859-871.

2. Zhou, T.; Commodore, L.; Huang, W.-S.; Wang, Y.; Sawyer, T.; Shakespeare, W.; Clackson, T.; Zhu, X.; Dalgarno, D., Structural Analysis of DFG-in and DFG-out Dual Src-Abl Inhibitors Sharing a Common Vinyl Purine Template. *Chem. Biol. Drug Des.* **2010**, 75, 18-28.

3. Estebanez-Perpina, E.; Arnold, L. A.; Nguyen, P.; Rodrigues, E. D.; Mar, E.; Bateman, R.; Pallai, P.; Shokat, K. M.; Baxter, J. D.; Guy, R. K.; Webb, P.; Fletterick, R. J., A Surface on the Androgen Receptor that Allosterically Regulates Coactivator Binding. *Proc. Natl. Acad. Sci. U.S.A.* **2007**, 104, 16074-16079.

4. May, P. C.; Dean, R. A.; Lowe, S. L.; Martenyi, F.; Sheehan, S. M.; Boggs, L. N.; Monk, S. A.; Mathes, B. M.; Mergott, D. J.; Watson, B. M.; Stout, S. L.; Timm, D. E.; Smith LaBell, E.; Gonzales, C. R.; Nakano, M.; Jhee, S. S.; Yen, M.; Ereshefsky, L.; Lindstrom, T. D.; Calligaro, D. O.; Cocke, P. J.; Greg Hall, D.; Friedrich, S.; Citron, M.; Audia, J. E., Robust Central Reduction of Amyloid-β in Humans with an Orally Available, Non-Peptidic β-Secretase Inhibitor. *J. Neurosci.* **2011**, 31, 16507-16516.

5. Ghosh, A. K.; Reddy, B. S.; Yen, Y. C.; Cardenas, E.; Rao, K. V.; Downs, D.; Huang, X.; Tang, J.; Mesecar, A. D., Design of Potent and Highly Selective Inhibitors for Human beta-Secretase 2 (Memapsin 1), a Target for Type 2 Diabetes. *Chemical Sci.* **2016**, 7, 3117-3122.

6. Wu, Y. J.; Guernon, J.; Rajamani, R.; Toyn, J. H.; Ahlijanian, M. K.; Albright, C. F.; Muckelbauer, J.; Chang, C.; Camac, D.; Macor, J. E.; Thompson, L. A., Discovery of Furo[2,3-d][1,3]thiazinamines as Beta Amyloid Cleaving Enzyme-1 (BACE1) Inhibitors. *Bioorg. Med. Chem. Lett.* **2016**, 26, 5729-5731.

7. Li, R.; Sirawaraporn, R.; Chitnumsub, P.; Sirawaraporn, W.; Wooden, J.; Athappilly, F.; Turley, S.; Hol, W. G., Three-Dimensional Structure of *M. tuberculosis* Dihydrofolate Reductase Reveals Opportunities for the Design of Novel Tuberculosis Drugs. *J. Mol. Biol.* **2000**, 295, 307-323.

8. Lam, T.; Hilgers, M. T.; Cunningham, M. L.; Kwan, B. P.; Nelson, K. J.; Brown-Driver, V.; Ong, V.; Trzoss, M.; Hough, G.; Shaw, K. J.; Finn, J., Structure-Based Design of New Dihydrofolate Reductase Antibacterial Agents: 7-(benzimidazol-1-yl)-2,4-diaminoquinazolines. *J. Med. Chem.* **2014**, 57, 651-668.